Ingénierie des Systèmes d'Information
Vol. 29, No. 1, February, 2024, pp. 141-146
Journal homepage: http://iieta.org/journals/isi

Neuronal Network-Founded Machine Knowledge with Pythons in Data Mining for Vast Information Classifications

Wasnaa K. Jawad*, Nada M. Kaittan, Bassam T. Sabri

Businesses Informatics College University of Information Technology and Communications, AlNidhal Campus, Baghdad 10001, Iraq

Corresponding Author Email: wasnaakadhim@uoitc.edu.iq

https://doi.org/10.18280/isi.290115

Received: 20 March 2023
Revised: 26 August 2023
Accepted: 31 December 2023
Available online: 27 February 2024

Keywords:
distributions on the big data, transform of the analytics, basic process of data mining, sectorize, the identification of review

ABSTRACT

Gesture recognition is a method for understanding the human body language through computers. This method bridges the gap between machines and humans more effectively than basic text or graphical user interfaces, or keyboard or mouse. Utilizing various mathematical techniques, the purpose of gesture recognition is to decipher the meaning behind human hand movements. It is possible for a gesture to come from any move or condition of the body, including the face or the hands. The dorsal hand veins are the focus of the study that is being done now in the area of hand gesture recognition. It has been shown via scientific research that the pattern of dorsal hand veins varies from person to person. When a person spins their hand in a certain way, the orientation of the vein pattern on their hand changes, revealing new veins. Such change in orientation is considered a gesture that should be measured. Subsequently, A gesture may be programmed to carry out a certain action. This method is especially helpful for people who have had damage to their spinal cord. The spinner handcuff is made up of a conventional of powers and sinews that are situated all everywhere the shoulder joint. Its primary function is to keep the top of the upper arm bone firmly anchored inside the shallow hollow of the shoulder blade. An injury to the rotator cuff may cause a dull aching in the shoulder, which is one of the symptoms.

1. INTRODUCTION

Acts and expressions of emotion are often represented by gestural symbols. Body and hand movements are also considered gestures. They may be broken down into two distinct classes: stationary and moving. In the former, a sign is sent by a person's physical position or the way they move their hands. The latter involves the use of hand and body movements to express ideas. Humans and computers may exchange information via the use of gestures. Unlike traditional hardware-based methods, gesture recognition can achieve human–computer interaction by determining user intent through the recognition of body or body part gestures or movements. Injuries to the rotator cuff are common among persons whose employment require them to conduct repetitive overhead movements or who participate in activities that require them to do so. Patients with rotator cuff injures will not be unable to perform certain tasks, such as steering a car. The solution to this issue is the use of gesture recognition, which will enable a driver to control the direction of a vehicle by just twisting his or her hand. An infrared camera has the ability to record the movement of a person's hand veins as they rotate. In this manner, an individual will not need to steer a car by traditional means. Its primary function is to keep the top of the upper arm bone firmly anchored inside the shallow hollow of the shoulder blade. An injury to the rotator cuff may cause a dull aching in the shoulder, which is one of the symptoms. Injuries to the spinner handcuff are common among persons whose employment require them to conduct repetitive overhead movements or who participate in activities that require them to do so. Patients with rotator cuff injures will not be unable to perform certain tasks, such as steering a car. The solution to this issue is the use of gesture recognition, which will enable a driver to control the direction of a vehicle by just twisting his or her hand. An infrared camera has the ability to record the movement of a person's hand veins as they rotate. In this manner, an individual will not need to steer a car by traditional means Because of its usefulness in areas as diverse as sign language recognition, augmented (virtual) reality, sign language clarification for persons with disabilities, and robot control, a great deal of effort has been put into improving hand gesture recognition technology.

2. THE PROPOSED METHOD

The spinner handcuff is made up of a established of powers and sinews that are situated all everywhere the shoulder joint. Its primary function is to keep the top of the upper arm bone firmly anchored inside the shallow hollow of the shoulder blade. A dull aching in the shoulder is one of the symptoms of a rotator cuff injury. This discomfort often becomes worse when the patient sleeps on the afflicted side, which is another one of the symptoms. Injuries to the rotator cuff are common

among painters, carpenters, and persons who play tennis and baseball, as well as other activities that require repetitive overhead movements [1-4]. Other common occupations associated with rotator cuff injuries include gymnasts and weight lifters. As one gets older, there is a greater chance of suffering an injury to the rotator cuff. Injuries to the rotator cuff may vary from mild irritation to full rips, depending on the degree of the injury. It is possible for a single injury to cause a tear in the rotator cuff [5-8]. It's no secret that rotator cuff injuries are painful, but they may also limit a patient's mobility. Both severe shoulder trauma and gradual tendon degeneration (wear and tear) may lead to rotator cuff illness. Fibers may become irritated or damaged if they are subjected to activities that include repeated overhead motions, extended lifting of large loads, or the formation of bone spurs around the elbow. Under such conditions, the patient will be unable to exert pressure on his/her shoulders. such as when steering the wheel while driving a car show in Figure 1.

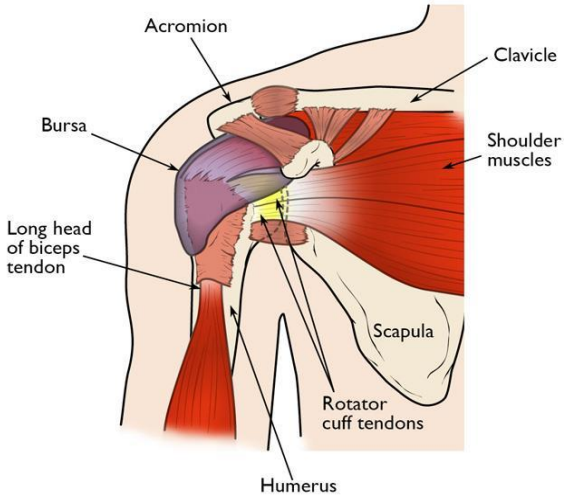

Figure 1. Diagram of rotary cuff

2.1 Abaxial hand attitudes

Biometry is rummage-sale in information security, which is a critical issue at present. Frequently used biometric technologies include fingerprint, retina, voice, and facial recognition systems. The biometric field is constantly being developed because of several drawbacks in various systems. The dorsal hand vein biometric system is a secure biometric scheme with minimal faults. Each person has their own one-of-a-kind pattern of veins on the palm of their hand [9-11]. Statistics show that only 6 in 1 million people share similar dorsal hand vein patterns, and thus, every single person has their own one-of-a-kind pattern. Due to the fact that hand veins are not visible to the human eye, dorsal hand vein detection is an extremely useful skill [12-14]. This form of identification also provides a clean system since it does not need physical touch. The fundamental features of a reliable biometric system are that it is steady across time, can be easily detected, is difficult to copy, provides correct results, and is really unique. All of these features are present in a system that can identify veins in the dorsum of a hand.

2.2 The identification and interpretation of hand signals

The purpose of this effort is to design an innovative method for the recognition of hand gestures. It is anticipated that the method will constitute a step toward the practical application of hand gesture recognition to everyday usage by putting out an altogether new algorithm in response to an existing issue.

The algorithm has to be able to fulfill the following requirements:

- flexibility
- practical precision, i.e., it can properly identify distinct signals 91%–101% of the while
- robustness, i.e., the system can successfully the ability to detect, track, and identify a variety of hand motions in a variety of illumination situations and crowded backdrops.
- robustness against scales and rotations
- scalability
- user-independent, i.e., the system should be applicable to various people rather than to a certain individual in particular. The system must be able to distinguish the hand movements made by a variety of human hands despite the fact that their sizes and hues will vary.

Dorsal hand vein recognition is user-independent and satisfies all the aforementioned conditions. In the current work, the orientation of dorsal hand veins is detected and used to steer a car accordingly.

2.3 Constituents' classification

only abbreviations firmly established in the field may be eligible. These keywords will be used for indexing pur Veins are not apparent to the human eye or to any other visual examination system because they are concealed under the surface of the skin. The data from the hand veins are acquired by the use of near-infrared (NIR) imaging technology, more specifically a monochrome NIR fee circuit (CCD) camera outfitted with an infrared (IR) lens. Two different infrared light sources are used to illuminate the back of the hand. Because the haemoglobin in the blood absorbs light from near-infrared light-emitting diodes (NIR LEDs), the venous system appears as a black network of lines. The Camera system is responsible for the recording of the pictures, which are then digitized, validated, and added to a database of registered images. Figures 2 provide illustrations of the dorsal veins of the hand [15-17].

Figure 2. Image of dorsal hand veins

3. METHOD

The processes that are involved in hand vein gesture tracking utilizing Kalman filtering. In the meanwhile, the procedures involved in the detection of hand vein gestures utilizing the discrete wavelet transform (DWT), the histogram of oriented gradients (HOG), and the reversible complex Hadamard transform are shown in Figure 2. The input picture is first transformed into a grayscale image, and then the area

of interest is extracted from the image (ROI). Following the completion of the image processing, a database is generated by rotating the pictures of the hand veins in both the clockwise and counterclockwise orientations. The database contains information on DWT, HOG, and four-phase reversible Hadamard transform, the latter two of which are methods [18-20].

- The tilt angle may be determined by first extracting features from the fragmented planes of the DWT, and then storing those features in the database for later matching.
- HOGs are first taken from the picture database, where they are then saved in the feature database before the rotated angle can be calculated.
- In order to discover the rotated angle and match features, features are first retrieved from the sectors of the inverse Hadamard wavelet transform and then saved in the database.
- Edge detection is calculated with the help of the Sobel and Canny operators in tracking that is based on Kalman filtering. Calculations are made to determine the reference centroid, and a Kalman filter is used on the track coordinates Figure 3.

The features obtained from the test image are likened with those from the database. The Euclidean coldness amid a comparison is made between the two photos after some kind of calculation has been performed. The optimal match is found at the shortest possible distance. The average, the middle value, the skewness, and the variance are the characteristics used (SD) [21-23].

During preprocessing, photos of hand vein patterns are trimmed to fit inside the requirements. ROI where veins appear prominent. The fingers are removed, and a uniformly adaptive histogram is constructed to adjust intensities. The The compiled database is then transformed into a training dataset.

One reduced (LL) sub-image, also known as a smoother picture, and three high-detail (LH), high-contrast (HL), and high-diagonal (HH) sub-images, respectively, constitute the whole image. By applying low-pass and high-pass decomposition filters to the source picture, DWTs breakdown is carried out in a pyramidal structure to yield four components with reduced resolution.

When compared with the input test image, the training set picture with the least feature vector distance is selected as the category for the input test image to be placed in. This selection is done by looking at all of the possible distances between the training set image and the input test image.

The DWT algorithm allows for the application of a wide variety of wave filters. The Daubechies, Coif lets, Samlets, and Fejer–Korovkin filters are all examples of different families of wavelets. This particular piece makes use of the Daubechies family name, Haar. A wavelet family or basis may be formed by a succession of rescaled square functions, which is what the Haar wavelet does. Following the application of the Haar transform, the DWT coefficients approximation, horizontal, vertical, and diagonal are produced. Additionally, the approximation coefficient is the most important of the four. When attempting to extract feature vectors, these coefficients are put to use [24-26].

3.1 Reversible complex Hadamard's convert

The complex Hadamards array H is an unidirectional matrix with entries -1 and -1, where j = -1. It has order N. In Eq. (1), this matrix is given in the following manner as follows:

$$HH^{*} = H * H = NI_{N} \tag{1}$$

where, H* denotes the complex conjugate transpose of matrix H. The matrix is an illustration of a complicated Hadamard array with a rank of 2. By using the Kronecker product in a recursive manner, it is possible to build higher-order complex Hadamards matrices [2, 5]. The following is an example of one such matrix, which may be found in Eq. (2) follows:

$$[CH]_{2^n} = [CH]_{2^{n-1}} \tag{2}$$

Direct and inverse reversible complex Hadamard matrices are presented in Eqs. (3)-(5) as follows:

$$[RC]_{2^n} = \left(\prod_{m=1}^{n=1} I_{2^{m-1}} * Q * I_{2^{n-m}}\right)(I_{2^{m-1}} * [CH]_2) \tag{3}$$

$$[RC]_{2^n}^{-1} = (I_{2^{n-1}} * [CH]_2^{-1})[\prod_{m=n-1}^{1} (I_{2^{m-1}} * Q^{-1}) \tag{4}$$

where,

$$f(\Sigma(Xl * Wl) + biase) \tag{5}$$

Direct and forward reversible complex Hadamard matrices of order 8 are presented in Eqs. (6)-(7), as follows in Figure 3:

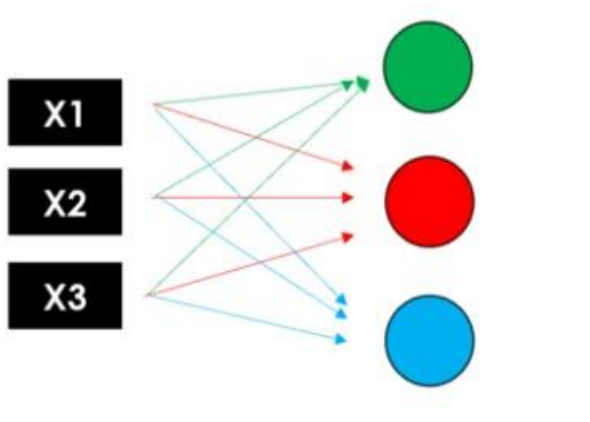

Figure 3. A dataset of N rows

The Walsh plan, a complicated space containing both real and fictitious parts, is segmented into circular sectors of 4, 8, and 12 degrees. To begin, let's split the complicated plane into quarters. When the number of sectors, say from 4 to 8 or 12 industries, the fundamental unit is the 4-sector airliner, and the criteria indicated in the relevant tables are used to carry out the sectorize [4, 19, 20]. Each industry is assigned its own unique feature representation. The average transform parameter for that area is represented by this vector. Because the sequence distribution of each hand picture varies among industries, this value is one-of-a-kind for each picture [27-29].

Each industry is assigned its own unique feature representation. Each industry's mean, standard deviation, deviation, and median are calculated. Since the distribution of each vein's sequence is variable between sectors, the values of these characteristics are also varied for each ridge and valleys. These numbers are much smaller than the transform coefficients or the vectors of technology assets features obtained by success of achieving. Thus, both processing time and complexity are decreased. The complicated 2D plane is partitioned into sectors using the parameters in Table 1.

Table 1. Subdivision data

Symbol of Sal +	Symbol of Cal +	Stage 00–900	Quadrantal Assigned I	Subdivision I
+	−	900–1900	II	II
−	−	1900–2800	III	III
−	+	2800–3700	IV	IV

When discussing the mean value of a stochastic process or a posterior distribution, the terms "mean" or "predicted value" are sometimes used interchangeably to refer to the same concept. The median is defined as the midpoint between the upper and lower halves of a data set, population, or posterior distribution. Because it has a breaking point of 50%, the mean is of paramount significance in 's paramount. The standard deviation of a probability density function for a real-valued random variable is a quantitative indicator of the amount of dispersion around the average. One may have a positive, negative, or undefined positively skewed value. The standard deviation (sometimes written as sigma,, or s) is a statistical metric used to express the degree of dispersion present in a given data collection [30-32].

3.2 Vein trailing by means of a Kalman's sieve

Monitoring a wide variety of objects moving is made easier with the assistance of the Kalman filter. The Kalman filtering technique is a technique that estimates the real present state of an item by combining noisy observations (and perhaps missing data) with predictions about the state of the object. A wide variety of linear dynamical systems are suitable candidates for implementation using Kalman filters [33-35]. In the context of this study, the term "state" may be used to refer to any quantifiable quantity, such as the position, velocity, heat, or voltage of an item, or even a mixture of many of parameters. The Kalman's sieve is a recruiting two phase sieve that is used in signal processing. At each iteration, it goes through the motions of predicting something and then revising that forecast. The present position of an item that is moving is estimated using data from earlier observations during the stage known as "prediction." For instance, if an item is travelling at a constant acceleration, then its present position may be estimated based on its prior location by using the equations of motion. This is possible because of the relationship between the two locations. In the updating stage, the observation of an object's current position, Zt (if it is available), is merged the foretold present site, Xt, to generate the posterior Ing projected present site of the item, Xt. This is done so that the material's location may be updated more accurately. Eqs. (6)-(9) determine how the Kalman filter operates (11).

Prediction stage: Predicted (a priori) state

$$X_k = F_k X_{k-1} + B_k U_k \tag{6}$$

Foretold (a priories) approximation covariances

$$P_{\frac{K}{K-1}} = F_K P_{(K-1)/(K-1)} F_K^T \tag{7}$$

As of instant t, the Kalman filter has generated an approximation of the vector field, denoted by XK. At instant t, we collect information along vector ZK. Reliability of XK prediction at time t is measured by PK. In the absence of noise, F defines the (ideal) transition of the systems from one condition to the next, or how one state vector is projected to the next (e.g., no acceleration). The relation H specifies between XK, the order to provide clarity, and ZK, the measure vector, is called a mapping. Q and R describe the system's variance as the Gaussian process and measurement noise, accordingly. The control input parameters B and u are only utilized by systems that need user intervention. In the case of an object tracker, these factors may be neglected [36].

3.3 Orientation of histogram

The look and form of a local item inside an image may be characterized using a Hog feature by analyzing the delivery of strength inclines or advantage instructions. A cell is a tiny linked section that may be used to break up a picture. A HOG is constructed for the individual pixels that make up each cell. The confluence of these sorts of histograms constitutes the descriptors. Local histograms may be stark difference to increase accuracy by measuring intensity over a wider section of an image known as a block. This calculation can be performed on many blocks. Then, this value is used to normalize all the cells within the block, thereby improving invaginating to vicissitudes in lighting and surveillance. A HOG signifier exhibits many advantages over other descriptors. First, it is invariant to geometric and photometric transformations, except for object orientation, given that it operates on local cells. These shifts never happen on a small scale; only on a global scale do we see such a phenomenon. As an added complication, pedestrians' unique body movements are ignored by coarse spatial sampling, fine orientation sampling, and robust local photoelectric normalization. provided that they remain in a roughly upright position. Thus, the HOG descriptor is particularly suitable for detecting humans in images.

The initial stage in the calculation process for image preprocessing in many feature detectors is to guarantee that the gamma and color values have been adjusted. In the process of computing the HOG descriptor, it is possible to skip this step since the normalization of the descriptor that follows accomplishes basically the same effect [20-22]. First, the values of the gradient are calculated. Applying a 1D centered, point discrete derivative mask in either or both the horizontal and vertical dimensions is the most typical way. This may be done in either or both of these directions. In specifically, in order to carry out this procedure, [23-25]. the hue or strength information of the picture must first be filtered using the filter kernels that are outlined in Eq. (8):

$$[-1 \quad 0 \quad 1] \; and \; [-1 \quad 0 \quad 1]^T \tag{8}$$

The average distance that may be measured between two locations is referred to as the Euclidean distance. Because there are no extra stages involved in the recognition process, this approach is not only straightforward but also very quick to compute. In addition, this approach is not affected by the shifting or rotation of fingerprint pictures.

Let x,y be the gray levels at location (k,l).

The Euclidean distance is presented by Eq. (9) as follows:

$$d_E^2 = \sum_{K=1}^{MN} (X^K - Y^K)^2 \tag{9}$$

4. RESULTS AND DISCUSSION

The images in the database that contain the hand images rotated clockwise and counterclockwise are shown in Figures 4 and 5, respectively. The hand pattern image is presented in Figure 5. The results of Kalman filtering using Sobel edge detection are presented in Figures 4 and 6.

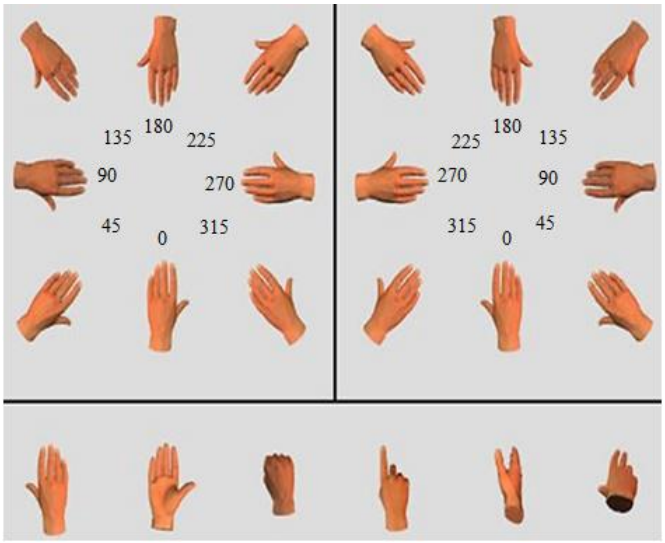

Figure 4. Database of hand images that are rotated clockwise

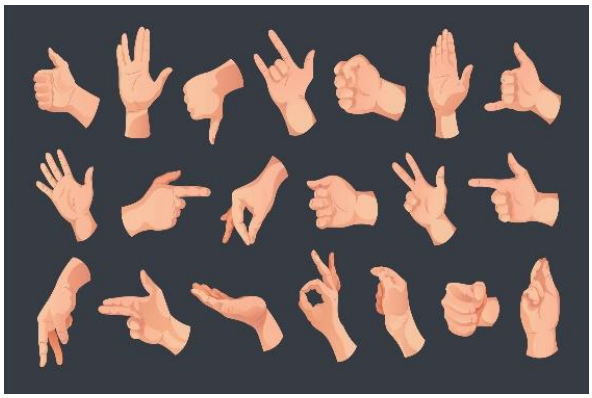

Figure 5. Database of hand images that are rotated counterclockwise

Figure 6. Input image

5. CONCLUSIONS

We have tested the algorithms over various rotations that range from −60° to 60°. We have successfully implemented the detection of various clockwise and counterclockwise rotations. We have implemented four methods for tracking hand rotation, namely, DWT, reverse Hadamard, HOG, and Gaussian filtration. We have found that each strategy yields very different outcomes. The accuracy of the results produced by each of these procedures varies. The comparison of the lengths of time required to carry out each of the procedures is shown in Table 2.

Table 2. Comparison of execution times

Algorithm	DWT	Reversible Complex Hadamard Transform	HOG
Time taken for execution (msec)	0.1130	0.1055	1.1266

We have determined that tracking the organizes of the orientation opinion using a Kalman filter achieves a precision of 26. The reversible four-phase complex Hadamard transform is the superior method because it takes the least execution time.

REFERENCES

[1] Jain, A.K., Mao, J., Mohiuddin, K.M. (1996). Artificial neural networks: A tutorial. Computer, 29(3): 31-44. https://doi.org/10.1109/2.485891

[2] Basu, J.K., Bhattacharyya, D., Kim, T.H. (2010). Use of artificial neural network in pattern recognition. International Journal of Software Engineering and Its Applications, 4(2): 23-33.

[3] Priyangga, H.Y., Ruliandi, D. (2018). Application of pattern recognition and classification using artificial neural network in geothermal operation. In Proceedings, 43rd Workshop on Geothermal Reservoir Engineering Stanford University, Stanford, California, pp. 1-9.

[4] Shang, C., Palmer, A., Sun, J., Chen, K.S., Lu, J., Bi, J. (2017). VIGAN: Missing view imputation with generative adversarial networks. In 2017 IEEE International conference on big data (Big Data), Boston, MA, USA, pp. 766-775. https://doi.org/10.1109/BigData.2017.8257992

[5] Bala, R., Kumar, D. (2017). Classification using ANN: A review. International Journal of Computational Intelligence Research, 13(7): 1811-1820.

[6] Nikzad, M., Movagharnejad, K., Talebnia, F. (2012). Comparative study between neural network model and mathematical models for prediction of glucose concentration during enzymatic hydrolysis. International Journal of Computer Applications, 56(1): 43-48.

[7] Sabri, B.T., Alhayani, B. (2022). Network page building methodical reviews using involuntary manuscript classification procedures founded on deep learning. In 2022 International Conference on Electrical, Computer, Communications and Mechatronics Engineering (ICECCME), Maldives, Maldives, pp. 1-8. https://doi.org/10.1109/ICECCME55909.2022.9988457

[8] Lazli, L., Boukadoum, M. (2013). Hidden neural network for complex pattern recognition: A comparison study with multi-neural network based approach. International Journal of Life Science and Medical Research, 3(6): 234-245. https://doi.org/10.5963/LSMR0306003

[9] Kepka, J. (1994). The current approaches in pattern recognition. Kybernetika, 30(2): 159-176.

[10] Sharma, P., Kaur, M. (2013). Classification in pattern recognition: A review. International Journal of Advanced Research in Computer Science and Software Engineering, 3(4): 298-306.
[11] Kattan, A., Abdullah, R. (2011). Training of feed-forward neural networks for pattern-classification applications using music inspired algorithm. International Journal of Computer Science and Information Security, 9(11): 44-57.
[12] He, S., Lau, R.W., Liu, W., Huang, Z., Yang, Q. (2015). Supercnn: A superpixelwise convolutional neural network for salient object detection. International Journal of Computer Vision, 115: 330-344. https://doi.org/10.1007/s11263-015-0822-0
[13] Ruiz-del-Solar, J., Loncomilla, P., Soto, N. (2018). A survey on deep learning methods for robot vision. arXiv preprint arXiv:1803.10862. https://doi.org/10.48550/arXiv.1803.10862
[14] Li, S., Deng, W. (2018). Deep facial expression recognition: A survey. arXiv preprint arXiv:1804.08348. https://doi.org/10.48550/arXiv.1804.08348
[15] Hasani, B., Mahoor, M.H. (2017). Facial expression recognition using enhanced deep 3D convolutional neural networks. In Proceedings of the IEEE Conference on Computer Vision and Pattern Recognition Workshops, pp. 30-40.
[16] Khorrami, P., Paine, T., Huang, T. (2015). Do deep neural networks learn facial action units when doing expression recognition?. In Proceedings of the IEEE International Conference on Computer Vision Workshops, pp. 19-27.
[17] Bargal, S.A., Barsoum, E., Ferrer, C.C., Zhang, C. (2016). Emotion recognition in the wild from videos using images. In Proceedings of the 18th ACM International Conference on Multimodal Interaction, pp. 433-436. https://doi.org/10.1145/2993148.2997627
[18] Vazquez, R. (2010). Izhikevich neuron model and its application in pattern recognition. Australian Journal of Intelligent Information Processing Systems, 11(1): 35-40.
[19] Hühnerbein, R., Savarino, F., Åström, F., Schnörr, C. (2018). Image labeling based on graphical models using wasserstein messages and geometric assignment. SIAM Journal on Imaging Sciences, 11(2): 1317-1362. https://doi.org/10.1137/17M1150669
[20] Zeng, X., Ouyang, W., Yan, J., Li, H., Xiao, T., Wang, K., Liu, Y., Zhou, Y., Yang, B., Wang, Z., Zhou, H., Wang, X. (2017). Crafting GBD-net for object detection. IEEE Transactions on Pattern Analysis and Machine Intelligence, 40(9): 2109-2123. https://doi.org/10.1109/TPAMI.2017.2745563
[21] Sala, P., Dickinson, S. (2015). 3-D volumetric shape abstraction from a single 2-D image. 2015 IEEE International Conference on Computer Vision Workshop (ICCVW), Santiago, Chile, pp. 796-804. https://doi.org/10.1109/ICCVW.2015.108
[22] Grauman, K. (2010). Efficiently searching for similar images. Communications of the ACM, 53(6): 84-94. https://doi.org/10.1145/1743546.1743570
[23] Dahikar, S.S., Rode, S.V. (2014). Agricultural crop yield prediction using artificial neural network approach. International Journal of Innovative Research in Electrical, Electronics, Instrumentation and Control Engineering, 2(1): 683-686.
[24] Jha, K., Doshi, A., Patel, P., Shah, M. (2019). A comprehensive review on automation in agriculture using artificial intelligence. Artificial Intelligence in Agriculture, 2: 1-12. https://doi.org/10.1016/j.aiia.2019.05.004
[25] Niedbała, G. (2019). Application of artificial neural networks for multi-criteria yield prediction of winter rapeseed. Sustainability, 11(2): 533. https://doi.org/10.3390/su11020533
[26] Liakos, K.G., Busato, P., Moshou, D., Pearson, S., Bochtis, D. (2018). Machine learning in agriculture: A review. Sensors, 18(8): 2674. https://doi.org/10.3390/s18082674
[27] Siegel, L. (1979). A procedure for using pattern classification techniques to obtain a voiced/unvoiced classifier. IEEE Transactions on Acoustics, Speech, and Signal Processing, 27(1): 83-89. https://doi.org/10.1109/TASSP.1979.1163186
[28] Khlebus, S.F., Hasoun, R.K., Sabri, B.T. (2022). A modification of the Cayley-Purser algorithm. International Journal of Nonlinear Analysis and Applications, 13(1): 707-716. https://doi.org/10.22075/ijnaa.2022.5559
[29] Sabri, B.T., Yaseen AL-Falahi, N.A., Salman, I.A. (2021). Option for optimal extraction to indicate recognition of gestures using the self-improvement of the micro genetic algorithm. International Journal of Nonlinear Analysis and Applications, 12(2): 2295-2302. https://doi.org/10.22075/ijnaa.2021.5375
[30] Hussein, R.R.A., Hamza, Z.F., Sabri, B.T. (2021). Forecasting the number of COVID-19 infections in Iraq using the ARIMA model. Journal of Applied Science and Engineering, 24(5): 729-734. https://doi.org/10.6180/jase.202110_24(5).0006
[31] Sabri, B.T. (2022). New approach exploring unclear weighted association rules using weighted support and trust framework by using data mining. International Journal of Intelligent Systems and Applications in Engineering, 10(3s): 100-112.
[32] Ali, B.S., Ucan, O.N. (2018). Lossy hyperspectral image compression based on intraband prediction and inter-band fractal. In Proceedings of the Fourth International Conference on Engineering & MIS 2018, pp. 1-10. https://doi.org/10.1145/3234698.3234705
[33] Fu, K.S. (1976). Pattern recognition and image processing. IEEE Transactions on Computers, 100(12): 1336-1346. https://doi.org/10.1109/TC.1976.1674602
[34] Sabri, B.T., Jawad, W.K. (2023). Discretion-preserving with data mining drive distribution scheme with a universal social grid web for vans using vast data. Ingénierie des Systèmes d'Information, 28(1): 211-216. https://doi.org/10.18280/isi.280124
[35] Qazi, K.A., Nawaz, T., Mehmood, Z., Rashid, M., Habib, H.A. (2018). A hybrid technique for speech segregation and classification using a sophisticated deep neural network. PloS One, 13(3): e0194151. https://doi.org/10.1371/journal.pone.0194151
[36] Sabri, B.T. (2022). A cutting-edge data mining approach for dynamic data replication that also involves the preventative deletion of data centres that are not compatible with one other. International Journal of Intelligent Systems and Applications in Engineering, 10(3s): 88-99.